Locus ceruleus controls Alzheimer's disease pathology by modulating microglial functions through norepinephrine

Michael T. Heneka[a,1], Fabian Nadrigny[b], Tommy Regen[c], Ana Martinez-Hernandez[d], Lucia Dumitrescu-Ozimek[a], Dick Terwel[a], Daniel Jardanhazi-Kurutz[e], Jochen Walter[a], Frank Kirchhoff[b,f], Uwe-Karsten Hanisch[c], and Markus P. Kummer[a]

[a]Deutsches Zentrum für Neurodegenerative Erkrankungen and Department of Neurology, University of Bonn, 53105 Bonn, Germany; [b]Neurogenetics, Max Planck Institute of Experimental Medicine, 37075 Göttingen, Germany; [c]Institute of Neuropathology, University of Göttingen, 37075 Göttingen, Germany; [d]Max Planck Institute of Biophysical Chemistry, Am Fassberg 11, 37077 Göttingen, Germany; [e]Bayer Schering Pharma, 13353 Berlin, Germany; and [f]Molecular Physiology, Institute of Physiology, University of Saarland, 66421 Homburg/Saar, Germany

Edited* by Tomas G. M. Hökfelt, Karolinska Institutet, Stockholm, Sweden, and approved February 16, 2010 (received for review August 21, 2009)

Locus ceruleus (LC)-supplied norepinephrine (NE) suppresses neuroinflammation in the brain. To elucidate the effect of LC degeneration and subsequent NE deficiency on Alzheimer's disease pathology, we evaluated NE effects on microglial key functions. NE stimulation of mouse microglia suppressed Aβ-induced cytokine and chemokine production and increased microglial migration and phagocytosis of Aβ. Induced degeneration of the locus ceruleus increased expression of inflammatory mediators in APP-transgenic mice and resulted in elevated Aβ deposition. In vivo laser microscopy confirmed a reduced recruitment of microglia to Aβ plaque sites and impaired microglial Aβ phagocytosis in NE-depleted APP-transgenic mice. Supplying the mice the norepinephrine precursor L-threo-DOPS restored microglial functions in NE-depleted mice. This indicates that decrease of NE in locus ceruleus projection areas facilitates the inflammatory reaction of microglial cells in AD and impairs microglial migration and phagocytosis, thereby contributing to reduced Aβ clearance. Consequently, therapies targeting microglial phagocytosis should be tested under NE depletion.

neuroinflammation | amyloid beta | neurodegeneration | phagocytosis

Alzheimer's disease (AD) is characterized by neocortical and hippocampal atrophy due to neuronal loss, the deposition of Aβ peptides, and the formation of neurofibrillar tangles. In addition, there is a progressive degeneration of cholinergic nuclei in the basal forebrain and of noradrenergic nuclei in the brainstem, most importantly the locus ceruleus (LC). This nucleus is the major source of norepinephrine (NE) supply in the mammalian brain. The LC provides the neurotransmitter via an extensive network of neuronal projections to all major brain regions. These regions include the neocortex and hippocampus, the seat of cognitive functions, learning, and memory.

Research dating back to the 1960s implicated LC degeneration in the pathogenesis of AD (1–3). Of particular relevance, several studies show that AD patients present with a prominent loss of LC cells, reaching 70% within the rostral nucleus and causing reduction of cortical and limbic NE levels (4). The drop in NE concentration tightly correlates with the progression and extent of memory dysfunction and cognitive impairment. Degeneration of LC neurons has been observed in patients exhibiting "mild cognitive impairment" (MCI) (5), an early form of AD, with 80% of MCI patients eventually succumbing to full AD (6).

Degeneration of LC neurons results in progressive loss of two different types of axons, those with either conventional synaptic contacts or varicosities. Varicosities are believed to release transmitter extrasynaptically into the microenvironment, where it may act on surrounding neurons, glial cells, and blood vessels (7). Locally diffusing NE is thought to execute additional functions apart from its role as a classical neurotransmitter. Indeed, NE negatively regulates transcription of inflammatory genes in astrocytes and microglia (8), both expressing functional adrenergic receptors (9). In addition, it has been shown, that this effect is mediated by β2-adrenergic receptors (9). Therefore, it has been proposed that NE serves also as an endogenous antiinflammatory agent.

We recently found that LC degeneration and NE deficiency modulate the level of Aβ deposition in an APP-transgenic mouse model of AD (10). In the present study, we test the role of NE as a positive regulator of microglial Aβ clearance in vitro and in vivo.

Results

NE Suppresses Microglial Transcription of Proinflammatory Genes. Exposure of microglial cells to fibrillar Aβ1–42 ($fA\beta_{1-42}$) for 4 h caused a rapid induction of proinflammatory gene transcription for TNFα, CCL2 (MCP1), iNOS, and COX2, whereas housekeeping genes L32 and GAPDH were not influenced. The presence of NE during the stimulation with $fA\beta_{1-42}$ almost completely abolished the inflammatory response (Fig. 1*A*). In vivo analysis of NE-deficient APP transgenic mice revealed a similar regulation of inflammatory gene transcription (Fig. S1).

NE Suppresses Microglial Cytokine and Chemokine Production. To extend the findings from the transcriptional level, we determined the influence of NE on a panel of cytokines and chemokines typically produced by activated microglia (9). NE or the β-adrenoreceptor agonist isoproterenol (Iso) induced a dose-dependent decrease in TNFα secretion (Fig. 1*B*). NE and isoproterenol also efficiently suppressed signals for the chemoattraction of monocytes (CCL2), Th1 cells (CCL3), and Th1/Th2 cells (CCL5) during Aβ stimulation (Fig. S2). These results are in accordance with our transcriptional analysis (Fig. 1*A*). Interestingly, the secretion of CXCL1 (KC, mouse equivalent of human GROα), which represents a signal for the recruitment of neutrophils, lymphocytes, and monocytes, was almost unaffected (Fig. 1*B* and Fig. S2). Immunohistochemical detection of astroglial and microglial reactivity in vivo showed that induction of NE deficiency increased GFAP expression and microglial activa-

Author contributions: M.T.H., F.N., F.K., U.-K.H., and M.P.K. designed research; M.T.H., F. N., T.R., A.M.-H., L.D.-O., D.J.-K., and M.P.K. performed research; M.T.H., F.N., T.R., A.M.-H., D.J.-K., F.K., U.-K.H., and M.P.K. analyzed data; and M.T.H., F.N., A.M.-H., D.T., D.J.-K., J.W., F.K., U.-K.H., and M.P.K. wrote the paper.

The authors declare no conflict of interest.

*This Direct Submission article had a prearranged editor.

Freely available online through the PNAS open access option.

[1]To whom correspondence should be addressed. E-mail: michael.heneka@ukb.uni-bonn.de.

This article contains supporting information online at www.pnas.org/cgi/content/full/0909586107/DCSupplemental.

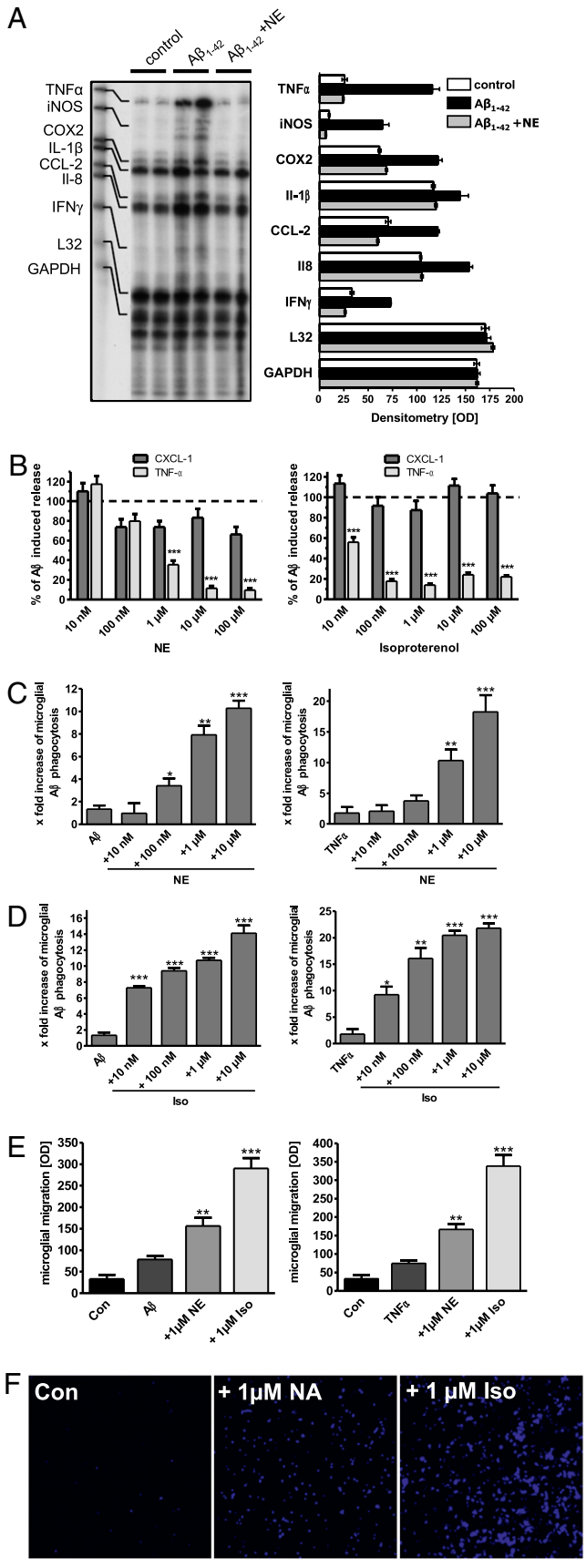

Fig. 1. Norepinephrine suppresses Aβ1–42-induced activation of primary murine microglial cells, and potentiates phagocytosis of Aβ and microglial cell migration. (*A*) Ribonuclease protection assay analysis of microglia for the expression of TNFα, iNOS, COX2, IL-1β, CCL2, IL-8, and INFγ under control conditions and stimulation with Aβ1–42 with or without NE coincubation for 2 h. L32 and GAPDH served as housekeeping control ($n = 8 \pm$ SE, performed in duplicate; **, $P < 0.01$; ***, $P < 0.001$, one-way ANOVA, Tukey's post hoc test). (*B*) Microglial cells were stimulated with 1 μM Aβ1–42 in the presence of increasing concentrations of NE (*Left*) or isoproterenol (*Right*). After 18 h, release of TNFα and CXCL1 was measured by ELISA ($n = 7 \pm$ SE; **, $P < 0.01$; ***, $P < 0.001$, one-way ANOVA, Tukey's post hoc test). (*C*) Microglia was either stimulated with 150 nM Aβ1–42 (*Left*) or 2 ng/mL TNFα (*Right*) for 30 min and thereafter exposed to a fluorescence-labeled, fibrillar Aβ1–42 (FITC-Aβ) with increasing concentrations of NE or isoproterenol (Iso) (*D*). Phagocytosis was assessed by FACS analysis ($n = 12 \pm$ SE; *, $P < 0.05$; **, $P < 0.01$; ***, $P < 0.001$, one-way ANOVA, Tukey's post hoc test). (*E*) Microglial migration was examined by Boyden chamber assay. Cells were either unstimulated (Con) or immunostimulated by Aβ1–42 or TNFα with or without NE or Iso ($n = 8 \pm$ SE; **, $P < 0.01$; ***, $P < 0.001$, one-way ANOVA, Tukey's post hoc test). (*F*) Visualization of migrated cells using DAPI. (Scale bar: 200 μm.)

tion (Fig. S3). Apparently, NE confers control over the microglial production of several immune mediators with distinct suppressive versus permissive outcomes. Stimulation of the β-subtypes is known to increase intracellular cAMP levels by adenylate cyclase activation. Indeed, microglial cells revealed a rapid and drastic increase in cAMP upon treatment with NE, indicating that NE acts in microglia through β-adrenoreceptors (Fig. S4).

Phagocytosis and Migration of Microglia Is Controlled by NE in Vitro. Analysis of microglial phagocytosis and migration in response to Aβ stimulation revealed that prestimulation of primary microglia by $A\beta_{1-42}$ (150 nM) or TNFα (1 ng/mL) (Fig. 1 *C* and *D*) only mildly increased the phagocytosis of fibrillar fluorescent-labeled $A\beta_{1-42}$ (FITC-Aβ). In contrast, simultaneous treatment of microglia with NE or Iso increased FITC-Aβ phagocytosis in a concentration-dependent manner (Fig. 1 *C* and *D*), resulting in a lysosomal localization of FITC-Aβ (Fig. S5). In addition, NE and Iso also augmented the migration of microglia in a Boyden chamber assay (Fig. 1 *E* and *F*). These data suggest that NE positively modulates key functions of microglia such as phagocytosis and migration.

NE Depletion Affects Aβ Burden Independent of APP Processing. To investigate whether NE interferes with the generation of Aβ peptides, we exposed a mouse neuroblastoma cell line stably overexpressing APP bearing the Swedish mutation (N2a APPsw) cells to NE in the presence or absence of the inflammatory cytokines TNFα and IL-1β. Detection of APP in cell lysates and secreted APPα or total Aβ in the supernatant of cells showed that APP processing was unaffected by NE, in the absence or presence of immunostimulation (Fig. 2*A*). Secretion of $A\beta_{1-42}$ and $A\beta_{1-40}$ was also unaffected as measured by sandwich ELISA (Fig. 2*B*).

To test our observation in vivo, we induced degeneration of aminergic LC neurons in APP-transgenic mice using the neurotoxin DSP4, which primarily affects LC axons and neurons but not the noradrenergic innervation arising from non-LC neurons (11). We observed a 70–80% reduction of NE in the forebrain of these mice and a strong reduction in tyrosine-hydroxylase immunoreactivity within the LC (Fig. S6). NE depletion resulted in an increase of extracellular Aβ deposition in the hippocampus and frontal cortex (Fig. 2*C*). In addition, we observed an increase in $A\beta_{1-42}$ in NE-depleted mice, whereas $A\beta_{1-40}$ was not changed (Fig. 2*D*). Levels of full length APP and C-terminal fragments were similar in both groups (Fig. 2*E*), suggesting that NE depletion inhibits phagocytosis of fibrillar $A\beta_{1-42}$ rather than altering the processing of APP.

NEUROSCIENCE

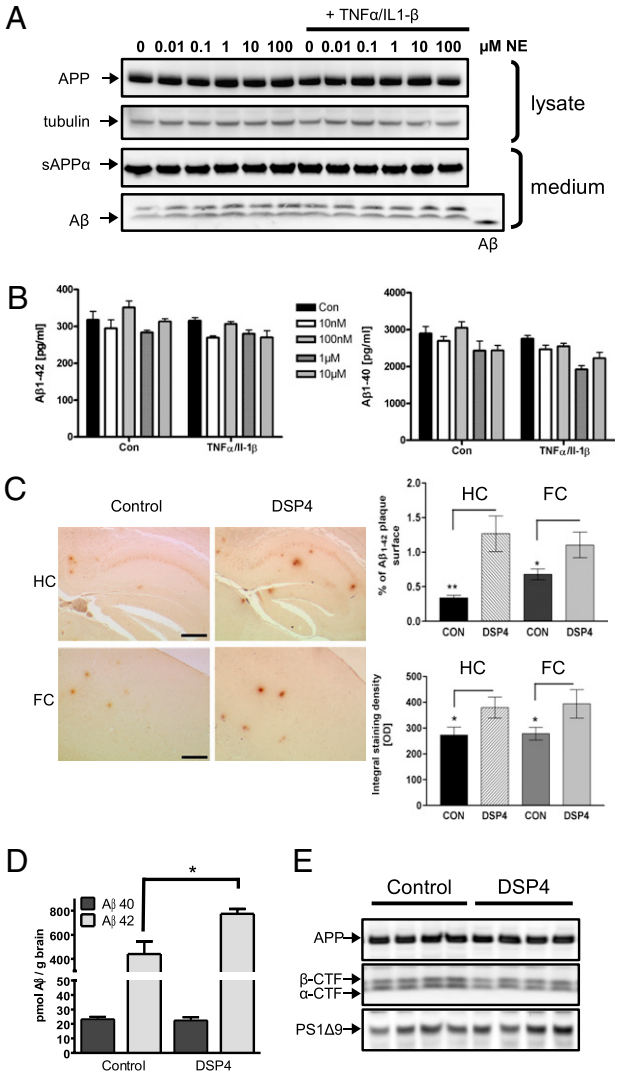

Fig. 2. Norepinephrine does not modify APP processing but modulates Aβ deposition in Alzheimer's disease mouse models. (*A*) N2a APPsw cells were incubated for 18 h with increasing concentrations of norepinephrine (NE) in the absence and presence of 1 ng/mL TNFα/IL-1β. Conditioned media were immunoblotted for Aβ and sAPPα by using antibody 6E10. APP and tubulin were detected in cell lysates by immunoblot with antibody 140 and E7, respectively. (*B*) Amounts of Aβ1–40 and Aβ1–42 in the conditioned media were quantified by sandwich ELISA. (*C*) Immunohistochemical analysis of Aβ deposition in 12-month-old APPV717I mice in response to noradrenergic depletion in the hippocampus (HC) and frontal cortex (FC) ($n = 10 \pm$ SE; *, $P < 0.05$; **, $P < 0.01$, Student's *t* test). (Scale bars: HC, 250 μm; FC, 100 μm.) (*D*) Noradrenergic depleted 6-month-old APP/PS-1 transgenic mice were analyzed for insoluble Aβ1–40 and Aβ1–42 by sandwich ELISA ($n = 7 \pm$ SE; *, $P < 0.05$, Student's *t* test). (*E*) Lysates of control and DSP4-treated mice were immunoblotted using antibodies against APP and presenilin 1.

NE Depletion Decreases Microglial Phagocytosis and Recruitment of Microglia to Amyloid Plaques. To assess microglial phagocytosis in vivo, we analyzed colocalization of Aβ deposits with the microglial activation marker CD11b in 12-month-old control and NE-depleted APP-transgenic mice. Aβ deposits were closely surrounded by CD11b-positive microglia (Fig. 3*A*). Although the number of CD11b-positive microglia increased along with the deposition, confocal microscopy showed that only a minority of microglial cells actually contained Aβ in NE-depleted animals (Fig. S7). Quantification of Aβ-containing microglia in DSP4-treated animals revealed a 70% decrease in colocalization (Fig. 3*B*).

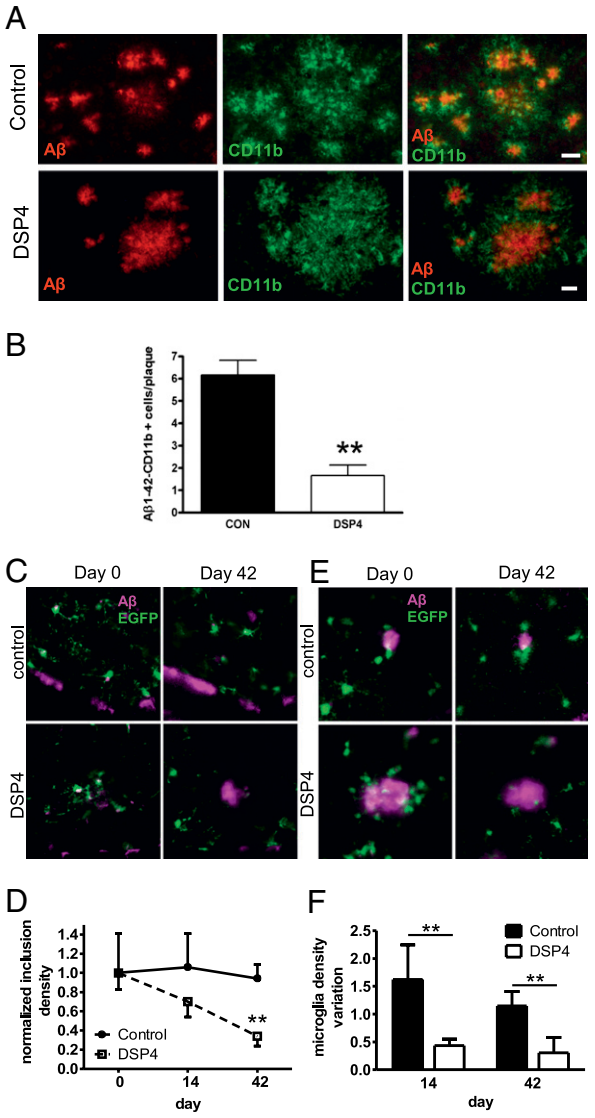

Fig. 3. NE depletion decreases microglial Aβ phagocytosis and results in reduced recruitment of microglia to Aβ plaques. (*A*) Confocal laser scanning microscopy detected a higher number of Aβ-plaque-associated and Aβ-containing microglial cells in 12-month-old APPV717I-transgenic mice compared to DSP4-treated mice. (Scale bars: 20 μm.) (*B*) Fifty randomly chosen plaques on 10 serial sections having a defined distance were evaluated for Aβ/Cd11b colocalization per animal ($n = 6 \pm$ SE; **, $P < 0.01$, Student's *t* test). (*C*) Example of plaques labeled with methoxy-X04 surrounded by EGFP expressing microglia at day 0 (*Upper Left*) and 42 (*Upper Right*). (*Lower*) Mouse treated with DSP4 at day 0 (*Lower Left*) and day 42 (*Lower Right*). Images are maximum intensity projection (MIPs) along the *z* axis. (Scale bar: 10 μm.) (*D*) Quantification of the temporal variation of the number of amyloid inclusions in microglia in different regions of control and DSP4-treated mice, respectively. Values are normalized by the median at day 0 ($n = 5$ for control and $n = 3$ for Dsp4-treated mice ± SE; **, $P < 0.01$, one-way ANOVA, Tukey's post hoc test). (*E*) Inclusions in microglia in the same region at day 0 (*Upper Left*) and day 42 (*Upper Right*). (*Lower*) Mouse treated with DSP4 at day 0 (*Lower Left*) and day 42 (*Lower Right*). Images are single optical sections. (Scale bar: 10 μm.) (*F*) Quantification of the variation of microglia density around plaques (in comparison with day 0) in control and DSP4-treated mice ($n = 5$ for control and $n = 2$ for Dsp4-treated mice ± SE; **, $P < 0.01$, Student's *t* test).

In addition, we crossbred APP-transgenic with CX_3CR1-EGFP knockin mice to monitor microglial reaction in NE-depleted mice colabeled with the amyloid dye methoxy-X04. Morphometric analysis (Fig. S8) revealed that the amount of Aβ inclusion within microglia was reduced after DSP4 treatment (Fig. 3 *C* and *D*). In

addition, we revealed reduced recruitment of microglia to amyloid plaques, suggesting that NE depletion also decreased attraction of microglial to amyloid deposits (Fig. 3 *E* and *F*). Taken together, NE depletion could promote amyloid plaque formation in vivo by inhibition of both recruitment of microglia to plaques and phagocytosis of Aβ.

Pharmacological Rescue of NE Levels in NE-Depleted APP-Transgenic Animals Restores Microglial Aβ Clearance. To further substantiate these findings, we conducted an adoptive transfer experiment by injecting primary murine microglial cells from CX_3CR1-EGFP-transgenic mice into the cortex of 16-month-old APPV717I-transgenic recipient mice cells (Fig. 4 *A* and *B*) with or without previous NE depletion by DSP4. After 24 h, brains were dissected and serial sections stained for $A\beta_{1-42}$. NE depletion caused a significant decrease of total migration distance of donor microglia as well as of Aβ positive microglial cells (Fig. 4*C*). Peripheral administration of the NE precursor L-threo-DOPS results in increased levels of NE within the cortex and hippocampus, as described in ref. 12. Importantly, treatment of APP-transgenic mice with L-threo-DOPS prevented the decrease of microglial migration and Aβ phagocytosis in NE-depleted mice (Fig. 4*C*). These results are in line with our in vitro findings (Fig. 1 *C*–*F*).

Discussion

LC degeneration and loss of LC-derived axons are associated with decreased NE levels in target forebrain regions in AD patients (4, 13, 14). Although these studies have assessed the loss of LC-noradrenergic neurons, it remains unclear when LC cell death starts and whether this structural degeneration is preceded by a significant period of dysfunction of noradrenergic LC neurons. However, the reduction of LC neurons positively correlates with Aβ plaque density, NFT numbers, and the severity of dementia (3). Importantly, the loss of LC neurons was found to be more extensive and to correlate better with the progression of AD than the cholinergic cell loss observed in the nucleus basalis of Meynert (15, 16). In contrast, compensatory mechanisms regarding NE levels in the CSF and the mRNA expression of α2-adrenoreceptors in the hippocampus of AD patients have been suggested (17–19). However, it is unclear whether increased NE measured form the CSF is congruent with the NE secreted from LC projection areas, but being produced in the brainstem or by terminally degenerated LC neurons.

Despite several neuropathological and clinical correlations that clearly indicate an association of LC impairment and noradrenergic degeneration with the extent of disease, it remained enigmatic how LC cell death influences AD pathogenesis.

Whereas NE contributes to normal acquisition, consolidation, and retention of certain learning tasks under physiological conditions (20), it has also been described as a potent antiinflammatory agent in several pathological paradigms (8). Although inflammation is basically a protective host response, uncontrolled or chronic inflammation can cause significant functional disturbance and structural damage—especially in a vulnerable tissue such as the CNS. NE would thus confer a strategic control over key immunoregulators, like TNFα, and serve as a gatekeeper for the emission of chemoattractants by local microglial populations.

Confirming and extending the cell-based findings by in vivo models, we show that chronic NE depletion in APP-transgenic mice increases the degree of neuroinflammation in areas usually innervated by LC. This finding suggests that the early degeneration of LC neurons and their terminals, which will result first in a local but later in an overall NE deficiency, may facilitate the inflammatory reaction in response to Aβ deposition in the AD brain. Given the fact that several inflammatory molecules have been found to impair neuronal functions that contribute to memory formation and consolidation, such as long-term potentiation (20–22), NE deficits may directly contribute to early neuronal dysfunction by subsequent elevation of inflammatory molecules. Next, it has been shown that proinflammatory cytokines, such as TNFα and IL-1β, can alone or in concert up-regulate the secretion of Aβ by increasing key players of the APP processing (23). Although we were not able to confirm this mechanism in this study,

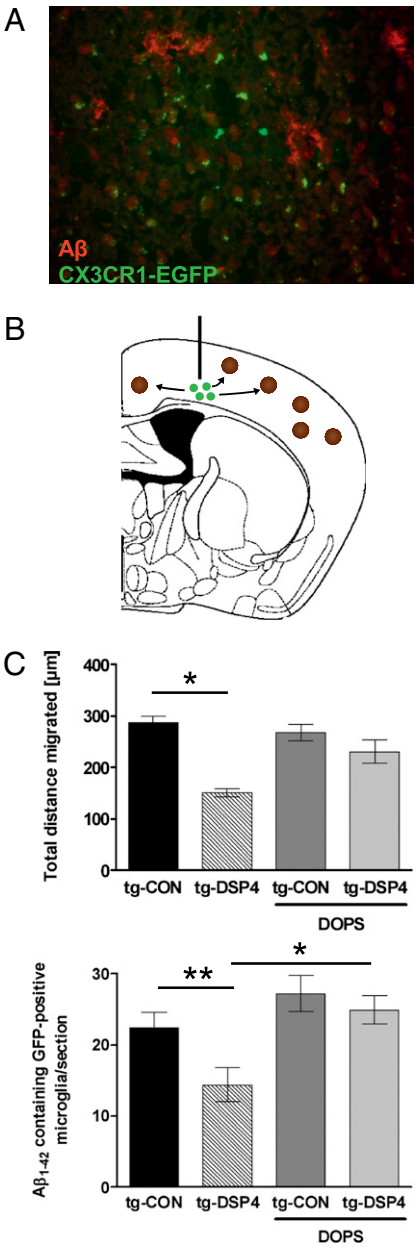

Fig. 4. Decrease of microglial migration after NE depletion in vivo is rescued by the NE-precursor L-threo-DOPS. (*A*) APPV717I-transgenic mice treated with DSP4 or solvent control received a single injection of primary murine microglia derived from CX3CR1-EGFP-transgenic mice. A subgroup of animals in both DSP4-treated and control groups received three i.p. injections of the NE precursor L-threo-DOPS (DOPS) over 24 h to increase NE levels within the neocortex. Shown is confocal laser scanning microscopy of Aβ plaques and EGFP-positive microglial cells. (Scale bar: 50 μM.) (*B*) Scheme of the intracerebral injection site depicting the migration of EGFP-positive microglial cells (green) toward amyloid plaques (brown). (*C*) The total distance migrated and the number of EGFP-positive microglial cells per section was evaluated by analyzing serial sections with a defined distance to each other and the injection site ($n = 6 \pm$ SE; *, $P < 0.05$; **, $P < 0.01$, one-way ANOVA, Tukey's post hoc test).

it cannot be fully excluded that LC degeneration may indirectly enhance the production of Aβ via its permissive effect on neuroinflammation.

Taken together, these data suggest that NE acts, beyond its role as a neurotransmitter, as an important regulator of microglial functions facilitating Aβ clearance. Migration to and phagocytosis of Aβ are likely to represent important cerebral decomposition mechanisms to respond to chronic Aβ deposition. In addition, other mechanisms of the neuroprotective effects of NE have been suggested. It has been shown that NE also acts on astrocytes resulting in the secretion of the neuroprotective chemokine MCP-1 (24) and that it is able to protect neurons from Aβ-induced damage involving PPARδ and GSH-synthesis (25).

Based on the findings of this study, one can hypothesize that LC degeneration favors the inflammatory reaction to Aβ while impairing its clearance at the same time—in particular, in a microenvironment where degeneration of a specific LC neuron and its projection has caused substantial drop of NE release. Even if remaining LC neurons show an increased activity in an attempt to compensate for the ongoing degeneration (17, 19), thereby generating at their terminals locally high NE levels, it seems likely that progressive LC degeneration may consequently cause neuroinflammation and a paralysis of phagocytotic clearance that first affects single spots but later the entire LC projection area. Such a chronic impairment of microglial Aβ clearance may ultimately contribute to the progression of the disease itself. Although abundant Aβ may drive proinflammatory cascades, the very depletion of NE lifts also the control over microglial proinflammatory release function affecting the major sentinels for homeostatic surveillance and maintenance (26).

It seems important to note that acute treatment of APP-transgenic mice with the NE precursor L-threo DOPS, which is in clinical use for the treatment of multiple system atrophy and depression, can reinstall the capacity of microglial cells to migrate and phagocytose Aβ, a phenomenon worth exploring therapeutically. Other therapeutic strategies targeting microglial functions, such as antibody-tag boosting of phagocytosis via vaccination against Aβ, should be evaluated in animal models under conditions of noradrenergic depletion. Given the fact that NE suppresses brain inflammation and enhances Aβ phagocytosis at the same time, restoration of brain NE levels may exert a desirable effect and thereby support vaccination strategies in AD.

Methods

Animals. Ten-month-old female APPV717I-transgenic mice (27) and 6-month-old female APP/PS-1-transgenic mice (28) were used. For the DSP4 treatment, we followed our published protocol (10), meaning that the initiation of any DSP4 treatment experiment consisted of two DSP4 i.p. injections at days 1 and 7 at a concentration of 50 mg/kg. Thirty minutes before DSP4, animals received fluoxetine (10 mg/kg) to protect serotonergic fibers, thereby increasing the selectivity of DSP4 for noradrenergic neurons. There were no further i.p. administrations of DSP4, when animals were analyzed within 8 weeks after first dosage. For longer observational periods, animals received monthly injections of DSP4 (50 mg/kg) to inhibit noradrenergic compensatory mechanisms (29–31). For in vivo microscopy of microglia, we crossbred heterozygous C57BL/6 TgH(CX3CR1-EGFP) mice with APP/PS-1-transgenic mice. Mice were housed in groups of four under standard conditions with free access to food and water. Animal care and handling was performed according to the declaration of Helsinki and approved by local ethical committees.

Primary Cell Culture. Microglial cells were prepared as described in ref. 32.

Multiplex Ribonuclease Protection Assay (RPA). Primary murine microglia were exposed to $A\beta_{1-42}$ (aged at 37 °C for 3 days) for 2 h in the presence or absence of NE at 10 μM. Total RNA was extracted using the RNeasy mini kit (Qiagen). Multiplex RPA was performed using a customized BD RiboQuant RPA kit (BD Bioscience) according to the manufacturer's protocol. The customized multiprobe template set consisting of TNFα, iNOS, COX2, IL-1β, MCP-1, IL-8, IFNγ, L32, and GAPDH was used to generate antisense riboprobes labeled with [^{32}P] UTP using the RiboQuant in vitro transcription kit. RNA was hybridized for 16 h at 56 °C. Samples were treated with RNase A/T1 mixture and proteinase K, separated by 4.75% denaturing polyacrylamide gel electrophoresis, and blotted, and signals were detected by phosphoimaging.

APP Processing and Aβ Secretion. Neuro-2a cells stably overexpressing Swedish APP695 (N2a APPsw) (provided by G. Thinakaran, University of Chicago) were incubated for 18 h in medium containing increasing concentrations of NE (Sigma). Cells were lysed in 25 mM Tris·HCl (pH 7.5), 1% Triton X-100, and 150 mM NaCl on ice and afterward centrifuged at 20,000 × *g* for 15 min. Forebrains of 6-month-old mice were homogenized in PBS containing 1 mM EDTA and EGTA and protease inhibitor mixture, further extracted in RIPA buffer [25 mM Tris·HCl (pH 7.5), 150 mM NaCl, 1% Nonidet P-40, 0.5% NaDOC, 0.1% SDS], and centrifuged at 20,000 × *g* for 30 min, and the pellet was solubilized in 2% SDS, 25 mM Tris·HCl (pH 7.5). Samples were separated by NuPage and immunoblotted using antibodies 6E10 (Covance), antibody 140 (33), Anti-PS1-NT (Calbiochem), and antibody E7 (Developmental Studies Hybridoma Bank), followed by incubation with appropriate secondary antibodies. Immunoreactivity was detected by enhanced chemiluminescence reaction (Millipore).

Aβ ELISA. Quantification of Aβ was performed using human Amyloid β_{1-40} and β_{1-42} ELISA kits (The Genetics Company) according to the manufacturer's protocol.

Phagocytosis of FITC-Labeled Aβ. Microglial cells (5×10^6 per mL) were incubated with 150 nM FITC-labeled Aβ1–42 (FITC-Aβ) (Anaspec) for 4 h at 37 °C, and 100 nM to 10 μM NE or isoproterenol was added. Microglia were treated with 250 μg/mL trypsin/EDTA. Mean fluorescence intensity (MFI) was measured on a FACScan (Becton Dickinson). Microglial Aβ phagocytosis was verified by confocal laser scanning microscopy (LSM 510; Zeiss) using antibody MCA711 against CD11b (Serotec) and LysoTracker Red (Invitrogen).

Microglial Migration in Vitro. Migration of murine microglial cells was assessed using a Boyden chamber (AP48; NeuroProbe) with an 8-μm polycarbonate PVPF-filter (Osmonics) in the absence and presence of TNFα (1 ng/mL) or fibrillar $A\beta_{1-42}$ and coadministration of NE or isoproterenol (10 nM to 10 μM) in DMEM containing 2.5% FCS. Incubation was performed at 37 °C for 4 h. Cells on the upper surface of the filter were scraped off, and the filters were fixed in methanol, stained with DAPI, and counted using ImageJ.

Microglial Cytokine and Chemokine Induction. Primary microglial cells were stimulated in 96-well plates (15,000 cells per well) with aged $A\beta_{1-42}$ peptide at 1 μM for 18 h either in the absence or presence of increasing concentrations of NE or isoproterenol (10 nM to 100 μM) or in case of CCL-2, CCL-3, CCL-5 and IL-12 (IL-12p70, IL-23, IL-12p40 and IL-12p40$_2$) with 8.2 μM NE. Supernatants were analyzed for CXCL1 and TNFα, CCL-2, CCL-3, CCL-5, and IL-12 as described in ref. 9.

Immunohistochemistry. Immunohistochemistry was performed as described in refs. 10 and 34. Saggital sections were incubated with antibody 32020 against iNOS (1:100; Transduction Laboratories), antibody 160116401 against COX2, (Cayman Chemicals), antibody MCA711 against CD11b, (Serotec), antibody MAB 377 against neuN (Chemicon), anti-tyrosine-hydroxylase AB152 (Chemicon), antibody MAB360 against GFAP (Chemicon) and antibody 44–344 against $A\beta_{1-42}$ (BioSource International). Quantification of the cellular loss of LC neurons was carried out by manual cell counting using merged images of TH-IR and DAPI stainings of the medial part of LC. The quantification of the TH-immunoreactive area of the LC was done using Cell^P (Olympus).

Quantification of Aβ Immunohistochemistry. For quantitative image analysis of hippocampal and cortical immunostaining, serial sagittal sections of one hemisphere of eight animals from each group were examined. For each animal, 20 parallel sections having a distance of 70 μm showing both the hippocampus and cortex were analyzed. Total stained area and integrated staining density (sum of all individual optical densities of each pixel in the area being measured) were determined and given as a percentage of stained area per region.

In Vivo Labeling of Aβ. 10 mg/kg methoxy-X04 [5 mg/mL in 50% DMSO, 50% NaCl (pH 12)] was injected i.p. 2 h before surgery (35). Surgery and imaging were performed under general volatile isoflurane anesthesia. Rectal tem-

perature was maintained between 36 and 38 °C. We used the thin-skull preparation using a drill (Fine Science Tool) over an area of 2 mm^2 above frontal cortex until the bone became flexible (50 μm thickness). After imaging, the skin was sutured and the mice were moved to a heated cage where they received i.p. and then s.c. injections of 0.05 mg/kg buprenorphine (Temgesic; Essex Pharma) every 8–12 h for 3 days. The whole procedure lasted <4 h.

In Vivo Imaging. To recognize the imaged site at each session, epifluorescence overviews of the cortex were acquired using a ×20, N.A. 1.0, water-immersion objective (Zeiss) and a CCD camera. High-resolution imaging was performed with a custom made two-photon laser scanning microscope (2P-LSM) equipped with an infrared fs-pulsed Ti:Sa laser (Chameleon Ultra; Coherent). ScanImage software (Version 3, Release 1) (36) was used to drive the 2P-LSM. To image amyloid deposits and microglia, we acquired *z*-stacks first at 750 nm (for methoxy-X04) and then at 925 nm (for EGFP). Optical filters were as follows: 735-nm long pass dichroic filter, 680-nm short pass emission filter, 750-nm long pass dichroic filter, and 510 ± 41-nm band pass filter (Semrock). The signal was collected by a photo-multiplier tube (Hamamatsu). Parallel, uniformly spaced (2–2.4 μm) planes of 120 × 120-μm^2 to 360 × 360-μm^2 regions of the frontal cortex were acquired, digitized, and processed to obtain *z*-stacks of images (512 × 512 pixels in size). Voxel size ranged from 0.23 × 0.23 × 2 μm^3 to 0.7 × 0.7 × 2.4 μm^3 regarding the *xyz*-axes. For quantification, see *SI Methods*.

Microglia Adoptive Transfer Experiments. Microglia was prepared at P1 from heterozygous CX3CR1-EGFP transgenic offspring, generated by targeted replacement of the *CX_3CR1* gene with the cDNA encoding EGFP (37). APPV717I-transgenic recipient treated with DSP4 or solvent control at 12 months of age received a single intracranial injection of primary murine microglial cells mice at 16 months of age. A subgroup of animals in the DSP4-treated and control groups received three i.p. injections of L-threo-DOPS over 24 h as described in ref. 12. For intracranial injection of cells, recipient mice were anesthetized with ketamine (30 mg/kg) and xylazine (4 mg/kg) and placed into a stereotaxic frame (Stoelting) maintaining body temperature at 37 °C. CX_3CR1-EGFP-positive microglial cells (5×10^3) in 5 μl were injected intracortically into the right hemisphere anteroposterior –2.5, lateral 2.0, and ventral 1.0 mm relative to the bregma at a rate of 1 μl/min. Twenty-four hours later, mice were killed and perfused with PBS, and their brains were removed. Ten-micrometer-thick serial cryosections (10 per mouse, $n = 8$) with a defined distance were stained for Aβ using antibody 2964 as described in ref. 33 and analyzed by confocal microscopy.

Statistical Analysis. Data were analyzed by using Student's *t* test, one-way ANOVA followed by Tukey's post hoc test, or two-way ANOVA followed by Bonferroni post hoc test using GraphPad Prism 5.

ACKNOWLEDGMENTS. We thank Dr. Heinz Steffens for his contribution to the in vivo imaging, Dr. Douglas Feinstein (University of Chicago) for critical reading of the manuscript, and Elke Pralle and Silke Strassenburg for excellent technical assistance. The monoclonal antibody E7 developed by M. Klymkowsky was obtained from the Developmental Studies Hybridoma Bank, developed under the auspices of the National Institute of Child Health and Human Development and maintained by the University of Iowa (Department of Biological Sciences). This work was supported by Deutsche Forschungsgemeinschaft Grants DFG-3350/4-1 (to M.T.H.), KFO177 (TP4) (to M.T.H.), and DFG-SFB-TRR43 (to U.-K.H. and F.K.), by the DFG-Research Center Molecular Physiology of the Brain (F.K.), and by Federal Ministry of Education and Research Grant 01GI0720 (to M.T.H.).

1. Forno L (1966) Pathology of Parkinsonism: A preliminary report of 24 cases. *J Neurosurg* (Supplement, Part II):266–271.
2. Iversen LL, et al. (1983) Loss of pigmented dopamine-beta-hydroxylase positive cells from locus coeruleus in senile dementia of Alzheimer's type. *Neurosci Lett* 39:95–100.
3. Bondareff W, et al. (1987) Neuronal degeneration in locus ceruleus and cortical correlates of Alzheimer disease. *Alzheimer Dis Assoc Disord* 1:256–262.
4. Matthews KL, et al. (2002) Noradrenergic changes, aggressive behavior, and cognition in patients with dementia. *Biol Psychiatry* 51:407–416.
5. Grudzien A, et al. (2007) Locus coeruleus neurofibrillary degeneration in aging, mild cognitive impairment and early Alzheimer's disease. *Neurobiol Aging* 28:327–335.
6. Petersen RC, et al. (2001) Current concepts in mild cognitive impairment. *Arch Neurol* 58:1985–1992.
7. Marien MR, Colpaert FC, Rosenquist AC (2004) Noradrenergic mechanisms in neurodegenerative diseases: a theory. *Brain Res Brain Res Rev* 45:38–78.
8. Feinstein DL, et al. (2002) Noradrenergic regulation of inflammatory gene expression in brain. *Neurochem Int* 41:357–365.
9. Mori K, et al. (2002) Effects of norepinephrine on rat cultured microglial cells that express alpha1, alpha2, beta1 and beta2 adrenergic receptors. *Neuropharmacology* 43:1026–1034.
10. Heneka MT, et al. (2006) Locus ceruleus degeneration promotes Alzheimer pathogenesis in amyloid precursor protein 23 transgenic mice. *J Neurosci* 26: 1343–1354.
11. Fritschy JM, Grzanna R (1991) Selective effects of DSP-4 on locus coeruleus axons: are there pharmacologically different types of noradrenergic axons in the central nervous system? *Prog Brain Res* 88:257–268.
12. Thomas SA, Marck BT, Palmiter RD, Matsumoto AM (1998) Restoration of norepinephrine and reversal of phenotypes in mice lacking dopamine beta-hydroxylase. *J Neurochem* 70:2468–2476.
13. Adolfsson R, Gottfries CG, Roos BE, Winblad B (1979) Changes in the brain catecholamines in patients with dementia of Alzheimer type. *Br J Psychiatry* 135: 216–223.
14. Mann DM, Lincoln J, Yates PO, Stamp JE, Toper S (1980) Changes in the monoamine containing neurones of the human CNS in senile dementia. *Br J Psychiatry* 136: 533–541.
15. Förstl H, Levy R, Burns A, Luthert P, Cairns N (1994) Disproportionate loss of noradrenergic and cholinergic neurons as cause of depression in Alzheimer's disease—a hypothesis. *Pharmacopsychiatry* 27:11–15.
16. Zarow C, Lyness SA, Mortimer JA, Chui HC (2003) Neuronal loss is greater in the locus coeruleus than nucleus basalis and substantia nigra in Alzheimer and Parkinson diseases. *Arch Neurol* 60:337–341.
17. Raskind MA, Peskind ER, Holmes C, Goldstein DS (1999) Patterns of cerebrospinal fluid catechols support increased central noradrenergic responsiveness in aging and Alzheimer's disease. *Biol Psychiatry* 46:756–765.
18. Szot P, et al. (2006) Compensatory changes in the noradrenergic nervous system in the locus ceruleus and hippocampus of postmortem subjects with Alzheimer's disease and dementia with Lewy bodies. *J Neurosci* 26:467–478.
19. Hoogendijk WJ, et al. (1999) Increased activity of surviving locus ceruleus neurons in Alzheimer's disease. *Ann Neurol* 45:82–91.
20. Murchison CF, et al. (2004) A distinct role for norepinephrine in memory retrieval. *Cell* 117:131–143.
21. Tancredi V, et al. (1992) Tumor necrosis factor alters synaptic transmission in rat hippocampal slices. *Neurosci Lett* 146:176–178.
22. Tancredi V, et al. (2000) The inhibitory effects of interleukin-6 on synaptic plasticity in the rat hippocampus are associated with an inhibition of mitogen-activated protein kinase ERK. *J Neurochem* 75:634–643.
23. Blasko I, Marx F, Steiner E, Hartmann T, Grubeck-Loebenstein B (1999) TNFalpha plus IFNgamma induce the production of Alzheimer beta-amyloid peptides and decrease the secretion of APPs. *FASEB J* 13:63–68.
24. Madrigal JLM, Leza JC, Polak P, Kalinin S, Feinstein DL (2009) Astrocyte-derived MCP-1 mediates neuroprotective effects of noradrenaline. *J Neurosci* 29:263–267.
25. Madrigal JLM, Kalinin S, Richardson JC, Feinstein DL (2007) Neuroprotective actions of noradrenaline: effects on glutathione synthesis and activation of peroxisome proliferator activated receptor delta. *J Neurochem* 103:2092–2101.
26. Hanisch UK, Kettenmann H (2007) Microglia: active sensor and versatile effector cells in the normal and pathologic brain. *Nat Neurosci* 10:1387–1394.
27. Moechars D, et al. (1999) Early phenotypic changes in transgenic mice that overexpress different mutants of amyloid precursor protein in brain. *J Biol Chem* 274:6483–6492.
28. Jankowsky JL, et al. (2001) Co-expression of multiple transgenes in mouse CNS: a comparison of strategies. *Biomol Eng* 17:157–165.
29. Wolfman C, et al. (1994) Recovery of central noradrenergic neurons one year after the administration of the neurotoxin DSP4. *Neurochem Int* 25:395–400.
30. Puoliväli J, Pradier L, Riekkinen P, Jr (2000) Impaired recovery of noradrenaline levels in apolipoprotein E-deficient mice after N-(2-chloroethyl)-N-ethyl-2-bromobenzylamine lesion. *Neuroscience* 95:353–358.
31. Fritschy JM, Grzanna R (1992) Restoration of ascending noradrenergic projections by residual locus coeruleus neurons: compensatory response to neurotoxin-induced cell death in the adult rat brain. *J Comp Neurol* 321:421–441.
32. Hanisch UK, et al. (2004) The microglia-activating potential of thrombin: the protease is not involved in the induction of proinflammatory cytokines and chemokines. *J Biol Chem* 279:51880–51887.
33. Wahle T, et al. (2006) GGA1 is expressed in the human brain and affects the generation of amyloid beta-peptide. *J Neurosci* 26:12838–12846.
34. Heneka MT, et al. (2002) Noradrenergic depletion potentiates beta -amyloid-induced cortical inflammation: implications for Alzheimer's disease. *J Neurosci* 22:2434–2442.
35. Bolmont T, et al. (2008) Dynamics of the microglial/amyloid interaction indicate a role in plaque maintenance. *J Neurosci* 28:4283–4292.
36. Pologruto TA, Sabatini BL, Svoboda K (2003) ScanImage: flexible software for operating laser scanning microscopes. *Biomed Eng Online* 2:13.
37. Jung S, et al. (2000) Analysis of fractalkine receptor CX(3)CR1 function by targeted deletion and green fluorescent protein reporter gene insertion. *Mol Cell Biol* 20: 4106–4114.